Talanta 189 (2018) 517–526

Contents lists available at ScienceDirect

Talanta

journal homepage: www.elsevier.com/locate/talanta

Preparation and analytical application of novel thiol-functionalized solid extraction matrices: From mesoporous silica to hybrid monolithic capillary column

Ling-yu Zhao[a,1], Qing-yun Zhu[a,1], Xiao-qin Zhang[a], Yi-jun Chen[a], Li Mao[b], Hong-zhen Lian[a,*], Xin Hu[a,*]

[a] State Key Laboratory of Analytical Chemistry for Life Science, Collaborative Innovation Center of Chemistry for Life Sciences, School of Chemistry & Chemical Engineering and Center of Materials Analysis, Nanjing University, Nanjing 210023, China
[b] MOE Key Laboratory of Modern Toxicology, School of Public Health, Nanjing Medical University, Nanjing 211166, China

ARTICLE INFO

Keywords:
Mesoporous silica
Hybrid monolithic column
Thiol-functionalization
One-step
Arsenic
ICP-MS

ABSTRACT

A comprehensively comparative study of thiol-functionalized mesoporous silica and organic-inorganic hybrid monolithic column was reported, aiming at the separation and enrichment of inorganic arsenic. Thiol-functionalized mesoporous silica was synthesized based on the one-step co-condensation method. At the same time, a novel thiol-functionalized organic-inorganic hybrid monolithic column was synthesized using an unconventional ternary weak basic solvent system *via* one-step sol-gel process. The approach to prepare monolithic column through mild condition remarkably improved delamination phenomenon of thiol-functionalized hybrid monolithic column easily caused by conventional methods. As(III) can be selectively uptaken by the hybrid monolithic column and homemade syringe-based solid phase extraction device containing mesoporous silica through chelation in a wide range of pH, while As(V) cannot, and then the captured As(III) was eluted by 3% HNO_3 (v/v) with 0.01 mol L^{-1} KIO_3. Under the optimized conditions, the extraction recoveries were 91–102% and 93–103% for mesoporous silica and monolithic column, respectively. Although both two materials were ideal solid matrices for the removal and speciation analysis of As(III) in environmental waters, the monolith-based solid phase microextration protocol was more fast and reagent-saving than the other, which endued monolithic columns with more application prospects for trace elemental analysis and speciation. Even so, the exploration of mesoporous silica could efficiently pilot the synthesis of monolithic columns.

1. Introduction

Trace metals exhibit widely different toxicities depending on their elemental species in the environment [1]. Arsenic, as a kind of main contaminate element of groundwater, soils and drinking water, derived from natural weathering of rocks, combustion of fossil fuel, the usage of arsenic pesticide and so on, has attracted major attention in large regions in the world [2,3]. The long-term exposure to arsenic-contaminated environment can cause many diseases, like dermatosis and the cancers of nasal passages and viscus [4]. The limited maximum concentration of arsenic stipulated by the World Health Organization is 10 μg L^{-1} in drinking water [5]. Arsenic exists in two predominant inorganic species, arsenite As(III) ($H_2AsO_3^-$, $HAsO_3^{2-}$ and AsO_3^{3-}) and arsenate As(V) ($H_2AsO_4^-$, $HAsO_4^{2-}$ and AsO_4^{3-}). As(III) is usually the dominant arsenic in environmental water. Because As(III) could react with mercapto group present in proteins, As(III) is usually more toxic and difficult to remove than As(V) [4,6,7]. Thus, separation and determination of As(III) and As(V) for the speciation analysis of arsenic is very necessary.

Solid phase microextraction (SPME), as a typical successful miniaturized sorbent-phase extraction technique, has been applied to element speciation studies by selective preconcentration, with a series of advantages such as high sensitivity, low sample requirement, low solvent consumption, simplicity, and easy automation [8]. Commonly used solid phase extraction (SPE) materials include polymer particles, biomass, carbon, zeolites, functionalized inorganic supports, mesoporous

* Correspondence to: School of Chemistry & Chemical Engineering and Center of Materials Analysis, Nanjing University, 163 Xianlin Avenue, Nanjing 210023, China.
E-mail addresses: hzlian@nju.edu.cn (H.-z. Lian), huxin@nju.edu.cn (X. Hu).
[1] These authors contributed equally to this work.

https://doi.org/10.1016/j.talanta.2018.07.034
Received 15 February 2018; Received in revised form 9 July 2018; Accepted 11 July 2018

silica, and capillary monolithic columns [9]. In contrast to some other solid materials, mesoporous silica and monolithic column as SPE/SPME matrices have attracted significant attention. Mesoporous silica has good dispersibility and controllable morphology, and shows a large adsorption capacity due to its large specific surface area [10]. Various functionalized mesoporous silicas with thiol, amine, phosphonate and so on, have been used for SPE to analyze heavy metals [10–13]. A small problem is that mesoporous material for SPE needs to achieve solid-liquid separation by centrifugation, which is a little tedious. To avoid this problem, we previously reported a homemade syringe-based SPE device containing thiol and amine-bifunctionalized mesoporous silica for the simultaneous uptake of As(III) and As(V) [9].

Capillary monolithic columns have been widely used for needle-SPME and on-line capillary solid phase microextraction (CME), because of their unique advantages, like uniform structure, controllable morphology, convective mass transfer and easy to automate [8]. Although the application of monolithic materials shows a great success in the area of organic and biological substances, it should be stressed that only a few applications have been reported on the analysis of trace elements and their speciation. For instance, Hu et al. proposed some methods based on capillary monolithic columns for CME-inductively coupled plasma mass spectrometer (ICP-MS) determination of trace elements. They connected two silica monolithic columns in series, which were respectively modified by amine and mercapto groups, to sequentially separate inorganic arsenic and selenium in natural water [14]. They also developed two kinds of functionalized polymer monolithic columns to analyze trace rare earth elements in human serum and urine samples [15,16], and proposed a TiO_2 NPs modified polymer monolithic column for the analysis of Gd^{3+} and Gd-diethylene triamine pentaacetic acid in human urine [17].

In comparison with classical inorganic silica and organic polymer monolithic columns, organic-inorganic hybrid monolithic columns prepared by a sol-gel reaction were preferred in some fields because of some advantages, such as large specific surface area, good biocompatibility and high mechanical stability [8,18]. In view of the special interaction of As(III) with mercapto groups, it will be a good choice to analyze As(III) using thiol-functionalized hybrid monolithic columns.

During the sol-gel reaction, silane reagents tend to hydrolyze under acidic conditions and polymerize under alkaline conditions. If the pH of pre-polymerization solution does not vary during the sol-gel process and silane reagents could hydrolyze and polymerize at the same time, this process would be called “one-step”. However, the presence of mercapto groups makes the solution acidic, which is difficult for silane reagents to polymerize. In the previous works, mercapto groups were generally introduced by post-modifying mercapto groups to the surface of prepared silica monoliths or hybrid monoliths with other active groups (such as vinyl) [14,19–21]. Mercapto groups only and unevenly exist on the surface of monoliths, and monolithic columns were hard to repeat through this kind of method. The other main method is to hydrolyze the pre-polymerization solution firstly under acidic or neutral condition at low temperature and then polymerize after adding basic solution inside [22–24]. Unfortunately, the polymerization process takes place in a very short period of time once the base is added, and there is no enough time to react with the inner wall of capillary, which easily makes monoliths not anchor tightly and requires high operator's skill. Here, we pay attention to preparation of an easy-to-prepared thiol-functionalized organic-inorganic hybrid monolithic column *via* “one-step”.

In fact, there are many similarities between mesoporous silica and hybrid monolithic column. Contrasting these two materials, same silane reagents were used in the synthesis process depending on the similar reaction mechanism. The difference is that mesoporous silica has more ways to characterize the framework structure and the successful introduction of functional groups because they are synthesized in vitro, however, the monolithic column materials need to be characterized after removal from the capillary, during which the backbone structure would be destroyed, and some characterization data are not accurate enough. The characterization results and synthesis conditions of functionalized mesoporous silica can provide inspiring reference for the preparation of organic-inorganic hybrid monolithic columns decorated by the same functional groups.

In this present work, we synthesized a thiol-functionalized hybrid monolithic column under unconventional ternary weak basic solvent system by a one-step procedure. Meanwhile, thiol-functionalized mesoporous silica was also prepared and used to fabricate a homemade syringe-based SPE device. Both the syringe-based SPE devices and monolithic column could selectively adsorb As(III) and therefore be used for separating and enriching As(III) in environmental water excluding As(V) interference, while the needle-SPME by thiol-functionalized hybrid monolithic column is better comparing with syringe-based SPE device. To the best of our knowledge, this is the first time to contrast the preparation and analytical application of mesoporous silica and hybrid monolithic column in one work.

2. Experimental section

2.1. Reagents and solutions

Cetyltrimethylammonium bromide (CTAB) was brought from TCI (Tokyo, Japan). Tetraethylorthosilicate (TEOS) and 3-mercaptopropyltrimethoxysilane (MPTMS) were purchased from Alfa Aesar (Tianjin, China). Sodium hydroxide (NaOH) was got from Nanjing Chemical Reagent Co. Ltd. Hydrogen nitrate (HNO_3) was of guaranteed reagent grade and obtained from Merck (Zurich, Switzerland). Isopropanol (IPA) and ethanol were purchased from Nanjing WanQing Chemical Glassware & Instrument Co. Ltd. Other chemicals were of analytical reagent grade and used without further purification. Deionized water (DIW) of 18.25 MΩ cm collected from a Milli-Q water system (Millipore, Bedford, MA, USA) was used throughout the experiment.

1000.0 mg L^{-1} stock solutions of inorganic As(III) and As(V), respectively, were prepared by dissolving Na_3AsO_3 and As_2O_5 (both of analytical reagent grade, purchased from Johnson Matthey, UK) in DIW. Lower concentration solutions were prepared daily by diluting the stock solutions with DIW.

Rain water was contained in our lab in the downtown campus located in Gulou District, Nanjing. River water was collected from Qinhuai River in Gulou District, Nanjing. Each environment water was filtered through a 0.45 μm cellulose acetate membrane before used.

2.2. Preparation of thiol-functionalized mesoporous silica and syringe-based SPE device

The thiol-functionalized mesoporous silica was prepared as followed (Scheme 1). In detail, 0.5 g of surfactant, CTAB, as the template, and 3.5 mL NaOH (1.0 mol L^{-1}) were dissolved in 120 mL DIW in a 250 mL 3-neck round bottom flask. The reaction system was stirred for 20 min at 80 °C. After the solution became clarified, a mixture of TEOS and MPTMS was dropped in using a pump (Baoding Longer, Model BT100) as impulse. After 10 min, fine white solid materials were obtained. The reaction mixture was stirred for another 2 h at 300 rpm under a nitrogen atmosphere. The resulting white powders were isolated by filtration under reduced pressure, washed with DIW (3 × 5 mL) and ethanol (3 × 5 mL), and then dried overnight at room temperature. The dried solid was added into a solution of ethanol and 1 mol L^{-1} HCl (1 g of synthesized material in 100 mL ethanol with 0.5 mL HCl) refluxing for 48 h at 80 °C to remove CTAB. After washed with DIW until neutral, the material was rinsed with ethanol and dried overnight at room temperature. In order to evaluate the influence of the molar ratio of MPTMS to silane reagents in the reaction system, the molar composition of the reaction mixture was set to (1-*x*) TEOS: *x* MPTMS: 0.11 CTAB: 0.28 NaOH: 532H_2O. Then, five thiol-functionalized mesoporous silica products, which were labeled as TFMS1 to

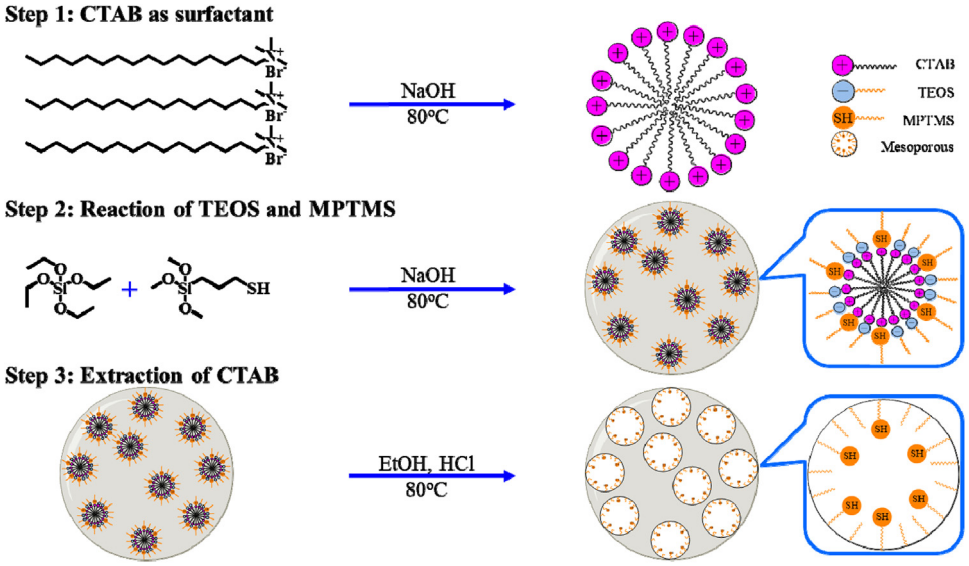

Scheme 1. Preparation of thiol-functionalized mesoporous silica.

TFMS5 respectively, were obtained with different *x* (0, 0.05, 0.1, 0.15 and 0.3).

A simple SPE device was fabricated with a syringe filter disc (0.45 μm) of 13 mm diameter, which was purchased from Jin Teng (Tianjin, China). Specifically, after the suspension containing 20 mg mesoporous silica and 1 mL DIW was injected into a syringe filter disc, thiol-functionalized mesoporous silica was uniformly collected on the filter membrane of syringe filter disc but DIW flowed out. Thus, a syringe-based SPE device with certain content of mesoporous silica was assembled successfully.

2.3. Preparation of thiol-functionalized hybrid monolithic capillary column

The monolithic columns were prepared (Scheme 2) in a fused-silica capillary with 530 μm i.d. and 690 μm o.d. (Reafine Chromatography Ltd., Hebei, China). To make sure the silanol groups on the inner wall of capillary activated enough, the capillaries were washed with 1 mol L^{-1} NaOH (12 h), DIW (30 min), 1 mol L^{-1} HCl (12 h), DIW (30 min) and methanol (30 min) at ambient temperature, and then dried under nitrogen flow for 24 h before used.

The thiol-functionalized monolithic columns were prepared from a solution containing ethanol, IPA, dilute ammonia, CTAB, TEOS and MPTMS. The optimal preparation conditions were as follows. Briefly, 33.3 mg CTAB were dissolved in a ternary weak basic solvent system constituted by 130 μL ethanol, 173 μL IPA, 152 μL 10% $NH_3{\cdot}H_2O$ solution (v/v). Subsequently, 300 μL TEOS and 100 μL MPTMS were added into the above mixture followed by vortexing at room temperature for 30 s and ultrasonication at 0 °C with ice for 30 s. The mixture was then pumped into the activated capillary with a certain length by a syringe. The capillary was placed in a 45 °C water bath to further react for 20 h after sealing the both ends with silicone rubber. After cooling to room temperature, the as-prepared monolithic column was syringed with methanol and DIW in turn to remove unreacted compounds, and then stored in 4 °C refrigerator. In the end, the long capillary containing a continuous monolith was cut into short pieces of 5 cm length for SPME.

2.4. Characterization of thiol-functionalized mesoporous silica and hybrid monolithic capillary column

The elemental analysis (EA) was carried out to investigate sulfur contents of mesoporous silica and monolithic column with an Elementar Vario EL III using oxygen as the combustion gas. Characterization of mercapto groups was carried out by Fourier transform infrared spectroscopy (FT-IR) and Raman spectra recorded respectively on Nicolet-6700 spectrometer and WITec alpha 300R confocal Raman system. Hitachi S-3400N II was used at an accelerating voltage of 10 kV for acquiring the scanning electron microscopy (SEM) morphology images and energy disperse spectroscopy (EDS) spectra of materials.

More than that, thermogravimetric analysis (TGA) and differential scanning calorimeter (DSC) were employed for the thermal analysis of the thiol-functionalized mesoporous silica on a Perkin-Elmer Pyris 1 DSC from 303 to 973 K with a heating rate of 10 K min^{-1}. X-ray diffraction (XRD) results of mesoporous silicas were performed with Philip X'Pert Pro using a Cu Kα radiation source and within the 2-theta range from 1.0° to 6.0°. N_2 adsorption-desorption measurement was carried out on a Micromeritics ASAP 2020 BET surface analyzer system at liquid N_2 temperature of − 196 °C. The surface area was calculated by using the Brunauer-Emmett-Teller (BET) equation, and pore size distribution was obtained by using the Barrett-Joyner-Halenda (BJH) model. The stereo structure of mesoporous silica, like mesoporous channel, was investigated by high resolution transmission electron microscopy (TEM) using a JEM-200CX microscope operating at a 200 kV accelerating voltage.

The measurement of As element (^{75}As) concentration in samples was conducted by ICP-MS (PerkinElmer ELAN 9000) system equipped

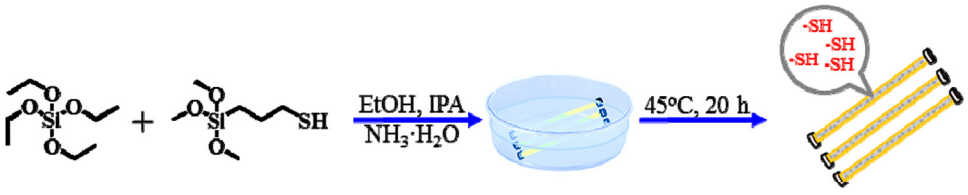

Scheme 2. Preparation of thiol-functionalized hybrid monolithic capillary column.

with a low flow rate micro concentric nebulizer (Glass Expansion, Switzerland). The optimized experimental parameters of the ICP-MS are listed in supporting information (Table S1).

2.5. Speciation analysis procedure

Thiol-functionalized mesoporous silica and monolithic capillary column were both used as SPE/SPME matrices during the As(III) speciation analysis procedure. Briefly, 4 mL As(III) solution was allowed to flow through the filter disc (SPE) at a flow rate of 20 μL min^{-1} or 5 cm monolithic capillary column (SPME) at a flow rate of 200 μL min^{-1} to uptake As(III), respectively. The flow rate of solution was precisely adjusted by the syringe infusion pump. In the elution step, 0.4 mL and 0.2 mL of 3% HNO_3 (v/v) with 0.01 mol L^{-1} KIO_3 were injected into the filter disc and monolithic capillary column respectively to desorb As (III). Centrifuge tubes were used for collecting effluents in speciation analysis procedure including loading and elution. Finally, all the effluents were introduced into ICP-MS for the determination of ^{75}As.

3. Results and discussion

3.1. Preparation and characterization of thiol-functionalized mesoporous silica and hybrid monolithic capillary column

3.1.1. Optimization of synthesis conditions for thiol-functionalized mesoporous silica

Fig. 1 showed XRD patterns in the region of 2θ = 1.0–6.0° for five thiol-functionalized mesoporous silicas. In diffractograms of TFMS1 to TFMS4, there were three clear characteristic peaks indexed as (1 0 0), (1 1 0) and (2 0 0) reflections, while peak intensity in the range of 2θ = 4.0–5.0° gradually weakened with the increase of MPTMS dosage. It could be clearly seen that TFMS5 did not exhibit any characteristic peaks associated with ordered mesoporous structure, which indicated that the attachment of excessive organic groups would destroy the structural order of mesoporous silica.

The physical characteristics of mesoporous silica, including N_2 adsorption-desorption isotherms and pore size distributions, are shown in Fig. 2A and B, respectively. The thiol-functionalized mesoporous silica TFMS1 to TFMS4 showed a type IV isotherm, which was a typical characteristic for mesoporous material. In contrast, TFMS5 exhibited no typical type IV isotherm. Meanwhile, the corresponding pore size distributions calculated by the BJH method presented the relatively narrow peak. The specific surface areas, pore sizes and pore volumes of these five materials are summarized in Table 1. As anticipated, TFMS1 to TFMS4 possessed high BET specific surface areas, pore sizes and pore volumes, while TFMS5 only displayed lower values.

The mesoporous structure and morphologies of mesoporous silica

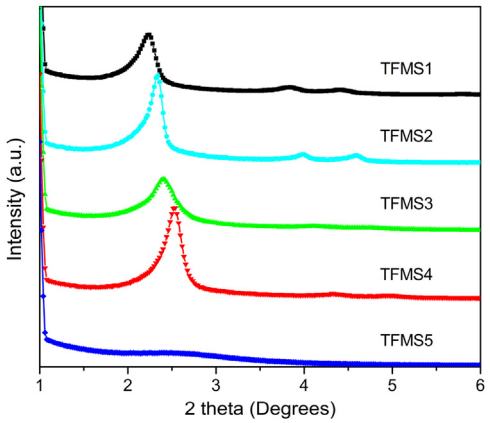

Fig. 1. XRD patterns of the thiol-functionalized mesoporous silicas (from TFMS1 to TFMS5).

TFMS1 to TFMS5 were further characterized by TEM and SEM, respectively. The TEM images of the five materials are presented in Fig. 3A. As expected, it could be seen that TFMS1 to TFMS4 possessed highly ordered pore structure, while TFMS5 did not. The results corresponded to XRD and BET well. The SEM micrographs of Fig. 3B revealed that TFMS1–TFMS4 were all composed of cashew nut particles, but exhibiting different particle sizes.

FT-IR spectra of five thiol-functionalized mesoporous silicas are plotted in Fig. 4A to confirm presence of some characteristic groups. Specifically, the bands at 2850–3000 cm^{-1} corresponded to C-H stretching. Besides, the weak absorption bands at around 2570 cm^{-1} were attributed to S-H stretching vibration. In order to further validate the successful grafting of mercapto groups on the mesoporous silicas, Raman spectroscopy was used for acquiring more distinct bands to confirm presence of mercapto groups. As can be seen in Fig. 4B, the band intensity at 2550–2590 cm^{-1} increased with increasing organosilane dosage.

In addition, EDS characterization of mercapto groups on the mesoporous silica is shown in Fig. 3C. The results also corresponded to EA as listed in Table S2. It was further found from the EA results that the ratio of sulfur content of the thiol-functionalized mesoporous silicas TFMS1 to TFMS5 increased concomitantly with the amount (x) of MPTMS from 0 to 0.3 in the composites. At the same time, thermal analysis, including TGA and DSC, were carried out for indicating organic matters (Fig. 2C and D). As shown in Fig. 2C, TFMS2 to TFMS4 all underwent a weight loss at 300–400 °C due to the decomposition of different content of mercapto groups. However, TFMS5 endured a more obvious weight loss in lower temperature ranges of 200–300 °C. This was possibly caused by incorporating excess organosilane which had not reacted completely in synthesizing the thiol-functionalized mesoporous silica. Therefore, free mercapto groups in residual MPTMS and thiol functional groups of mesoporous silica coexisted in system, which influenced the temperature ranges of weight loss. Besides, DSC was used for further providing evidence for the amount of mercapto groups. There were two sharp peaks in DSC curves of TFMS2 to TFMS5, respectively corresponding to the endothermic event at 100 °C and exothermic event at 350 °C, which was mainly due to decomposition of mercapto groups. As anticipated, it was observed that TFMS1 did not show characteristic weight loss and exothermic peak correspond to mercapto groups.

3.1.2. Optimization of synthesis conditions for thiol-functionalized hybrid monolithic column

We tried to prepare thiol-functionalized monoliths referencing previous work [22,25] and mesoporous silica in this work, but make some appropriate adjustments. In order to dissolve the silane reagents better and improve the void structure, IPA was added to the solvent system. Initially, TEOS and MPTMS were used as precursors, CTAB as template, ethanol, IPA and DIW as cosolvent and coporogen, and NaOH as basic catalyst for sol-gel process. However, after investigation, we found that this monolith had very weak adsorption capacity for As(III), even though the EDS and FT-IR results showed that the material was rich in sulfur element and mercapto groups. The main reason might be that NaOH as a strong base possibly corroded mercapto groups on the surface of material and internal mercapto groups were retained. So, NaOH was replaced by 10% $NH_3{\cdot}H_2O$ solution (v/v), which was relatively weakly basic, and the adsorption capacity for As(III) was enhanced significantly. Thereafter, the copolymerization reaction slowed and the resulting material was more homogeneous than before. After continuous optimization of conditions, the best solvent ratio was determined as ethanol: IPA: 10% $NH_3{\cdot}H_2O$ solution (v/v) = 130:173:152 (v/v/v).

Controlling the total silane reagent volume unchanged, the ratios of TEOS and MPTMS were adjusted to be TEOS: MPTMS = 340:60, 320:80, 300:100, 280:120 (v/v), from S1 to S4. It was seen clearly from FT-IR spectra (Fig. 5) that the higher the ratio of MPTMS, the more

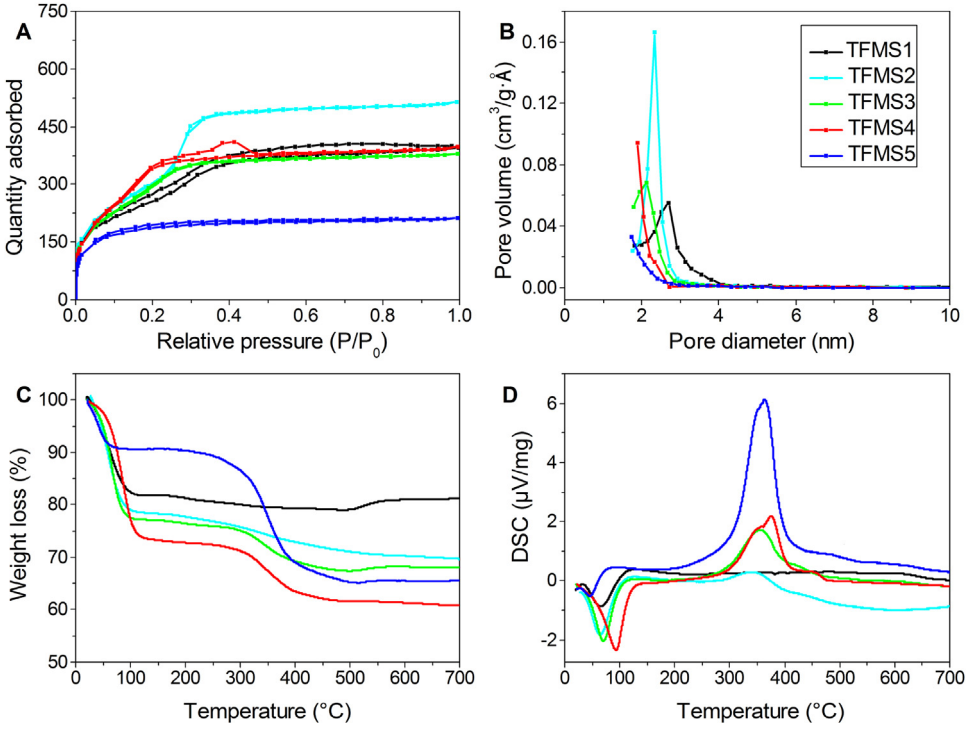

Fig. 2. N_2 adsorption-desorption isotherms (A), pore size distribution (B), TGA (C) and DSC (D) curves of the thiol-functionalized mesoporous silicas (from TFMS1 to TFMS5).

Table 1
The physical characteristics of the thiol-functionalized mesoporous silicas (from TFMS1 to TFMS5).

Material	S_{BET} ($m^2\ g^{-1}$)	Pore volume ($cm^3\ g^{-1}$)	Pore size (nm)
TFMS1	977	0.61	2.66
TFMS2	1137	0.79	2.37
TFMS3	1104	0.59	2.21
TFMS4	1131	0.62	2.22
TFMS5	628	0.33	2.16

pronounced the S-H stretching vibration (~ 2570 cm^{-1}), which meant the more mercapto groups. It was the same for mesoporous silica. However, when TEOS: MPTMS were lower than 280:120 (v/v), the skeleton structure of monoliths was very fragile. Finally, the ratio of TEOS and MPTMS was set to be 300:100 (v/v).

The morphology of thiol-functionalized hybrid monolithic column was characterized by SEM. From the SEM images of the columns shown in Fig. 6(1), it can be seen from the cross-sectional images that the monolith possessed a homogeneous microstructure and was anchored tightly to the inner wall of capillary without obvious voids, which facilitated the homogenous and quick mass-transfer during the sample preparation procedure. In addition, the continuous macroporous structures could result in high permeability and low backpressure. We recorded the pressure variation of the monolithic column with different flow rates of water. The column back-pressure was linearly increasing in the whole tested flow rate range, which indicated that the columns had good mechanical strength (Fig. S1). Meanwhile, the average BET surface area of thiol-functionalized monolithic column calculated by the BJH method was 68.51 $m^2\ g^{-1}$. As shown in Fig. 6(1)B and C, the well-controlled skeleton of the monolith was formed by continuous interconnecting spheres with rough surface, which was contributed to high surface area and good adsorption capacity of As(III). This was consistent with the result of average surface area.

The successful modification of mercapto groups on the monoliths was further verified by some other characterizations. Raman spectrum characteristic peak at ~ 2570 cm^{-1} of the monoliths was obvious to confirm the presence of mercapto groups (Fig. S2). The EDS result in Fig. 6(2) showed significant exists of sulfur element and the atomic concentration ratio of sulfur measured by EA also proved that the thiol-functionalized monolithic columns had been successfully synthesized (Table S3).

3.2. Optimization of speciation analysis procedure

3.2.1. Effect of pH on arsenic adsorption

On the basis of characterization results, the influence of pH on arsenic adsorption by TFMS1 to TFMS4 was studied with an initial concentration of 20 μg L^{-1} As(III) or As(V) solution (Fig. S3), while TFMS5 was not selected for its destroyed structural order as mentioned above. TFMS2-TFMS4 all showed excellent adsorption rate to As(III) through chelation, while TFMS1 only interacted weakly with As(III) due to nonspecific adsorption. In comparison, TFMS4 had more adsorption rate (> 90%) from pH 1.0 to 10.0 than that of TFMS2 and TFMS3. As discussed above, TFMS4 exhibited not only highly ordered mesoporous structure (high surface area and pore volume), but also the highest coverage of mercapto groups. As a result, TFMS4 was selected to be further studied and compared with thiol-functionalized hybrid monolithic capillary column.

The effect of pH on the adsorption of As(III) and As(V) onto the TFMS4 and monolith column are given in Fig. 7A and B respectively. It was apparent from these results that two absorbents both exhibited high adsorption rate to As(III) in the pH range of 1.0–10.0 except for very few points found in Fig. 7B. The lower adsorption rate around pH 2.0 and 3.0 was also reported in some other reported work, but the cause has not been clearly explained yet [26,27]. On the other hand, TFMS4 and monolith column did not show appreciable adsorption to As (V) as anticipated, because chelation between mercapto groups and As (III) rather than As(V) was very strong. Even so, monolith column still showed better adsorption selectivity for As(III) from inorganic arsenic within specific pH ranges of 4.0–10.0 for the fact that the adsorption rate of As(V) was almost zero. For confirming the selective adsorption

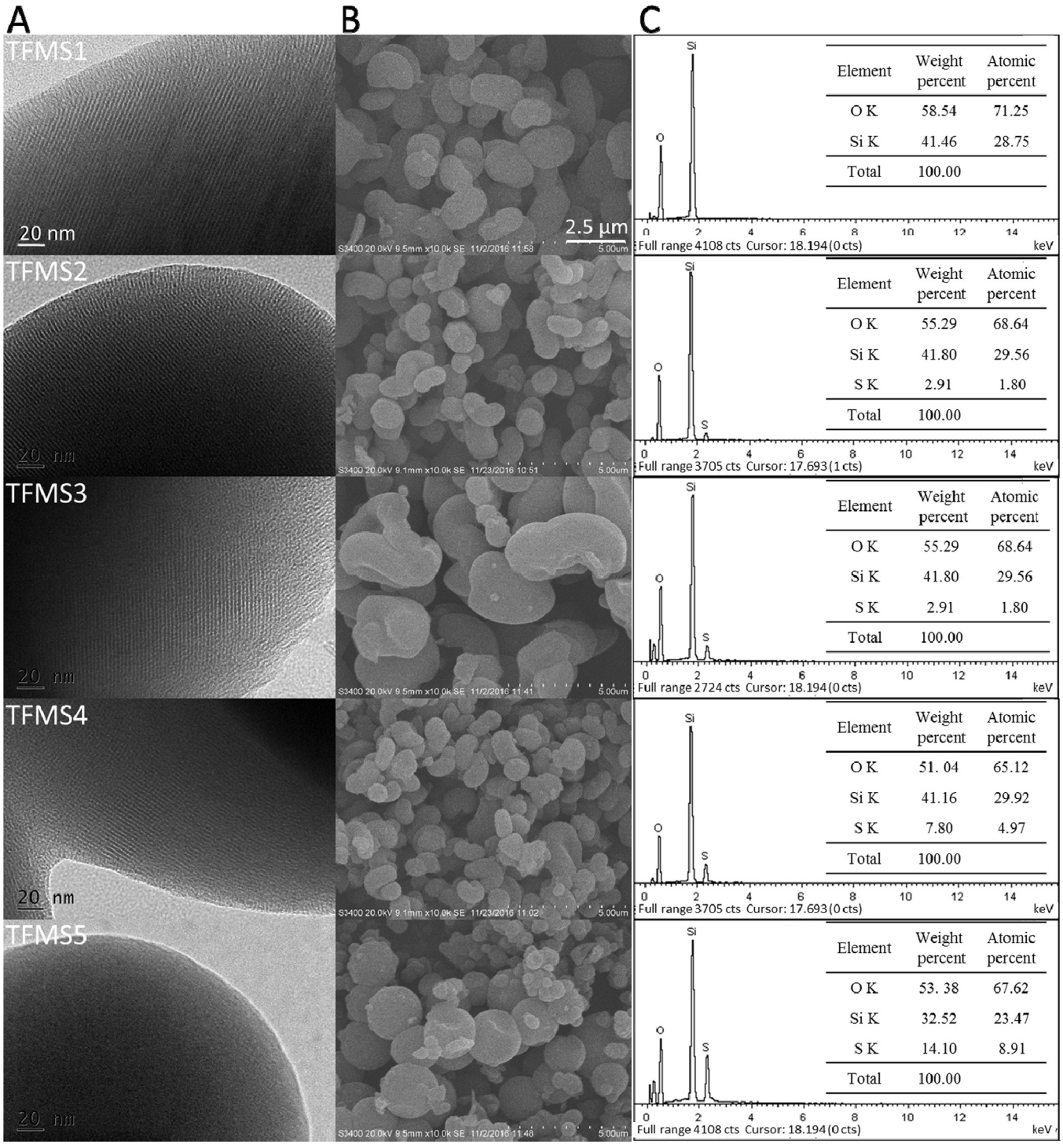

Fig. 3. SEM (A) and TEM (B) images and EDS results (C) of the thiol-functionalized mesoporous silicas (from TFMS1 to TFMS5).

of these two materials to As(III), we further implemented the EDS of adsorbents before and after soaking in As(V) or As(III) solutions (pH 4.0). It can be seen from Table S4 that only the presence of As can be detected in the adsorbents after soaking in As(III) solution. Therefore, the sample pH of 4.0 was selected for TFMS4 and monolith column in the subsequent experiments.

3.2.2. *Effect of flow rate*

Flow rate plays an important role in adsorption of As(III) on TFMS4 and monolith column as illustrated in Fig. 7C. Firstly, the effect of flow rate was studied by passing 1.0 mL As(III) solution (pH 4.0) through the syringe filter disc (introduced in Section 2.2) in range of 10–100 μL min^{-1}. It was found that the adsorption rate decreased when the flow rate was over 20 μL min^{-1}. Thus, a flow rate of 20 μL min^{-1} was selected as the optimum eluent flow rate for mesoporous silica syringe filter disc. Then, the similar experiment was performed by thiol-functional monolith column with different range of flow rate from 10 to 300 μL min^{-1}. By contrast, the adsorption rate was still high even though flow rate had reached 300 μL min^{-1}. Based on consideration of stability of the monolithic skeleton, 200 μL min^{-1} was selected for

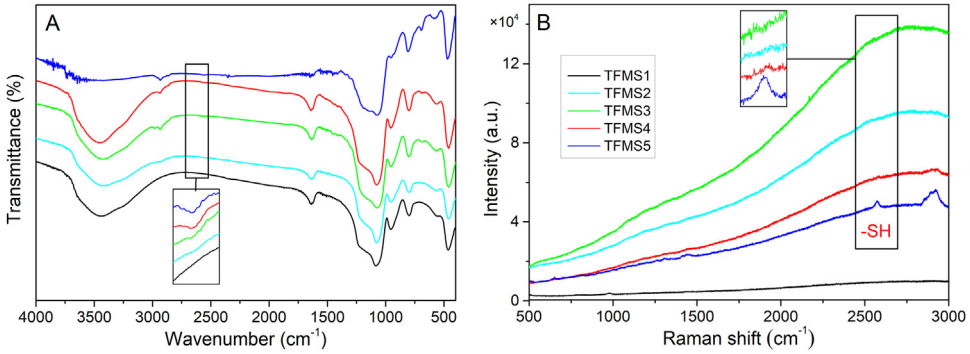

Fig. 4. FT-IR (A) and Raman (B) spectra of the thiol-functionalized mesoporous silicas (from TFMS1 to TFMS5).

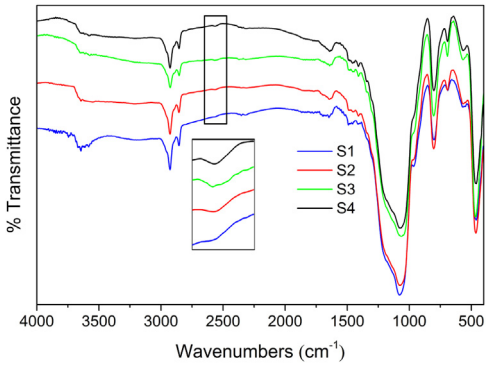

Fig. 5. FT-IR spectrum of the thiol-functionalized monolithic column.

subsequent experiments. Moreover, adsorption kinetics of As(III) onto TFMS4 by batch SPE is shown in Fig. S4. The equilibrium time took only 10 min, which indicated that the equilibrium process was very fast.

3.2.3. Effect of sample volume

The effects of 1.0, 2.0, 4.0 and 5.0 mL sample solution containing 50 ng As(III) were tested at the optimum pH and flow rate. The results of TFMS4 and monolith column are given in Fig. 7D. It was found that adsorption rate for As(III) was still between 95% and 100% in the range of 1.0–5.0 mL, which met the needs of the actual analysis. In order to save time, 4.0 mL was selected for subsequent experiments. The sample volume could be further expanded to get a larger enrichment factor, if neglecting the time.

3.2.4. Adsorption capacity

Adsorption capacity is an important factor in evaluating performance of adsorbent. The systemic study of adsorption capacity was carried out based on the method recommended by Hu et al. [28]: 5.0 mg L^{-1} As(III) solution was allowed to flow through the filter disc and 5 cm monolithic capillary column continuously under optimized conditions, and effluents were detected by ICP-MS. Adsorption capacities were calculated, when the increasing signal emerged suddenly, to be above 10.0 mg g^{-1} for thiol-functionalized mesoporous silica and 2.32 μg cm^{-1} (~ 3.01 mg g^{-1}) for the monolithic column. We also drew As(III) adsorption isotherms (Fig. S5). According to Langmuir adsorption isotherm models, the adsorption capacities of As(III) were 10.46 mg g^{-1} for thiol-functionalized mesoporous silica and 2.43 μg cm^{-1} (~ 3.15 mg g^{-1}) for the monolithic column, which were basically matched with above.

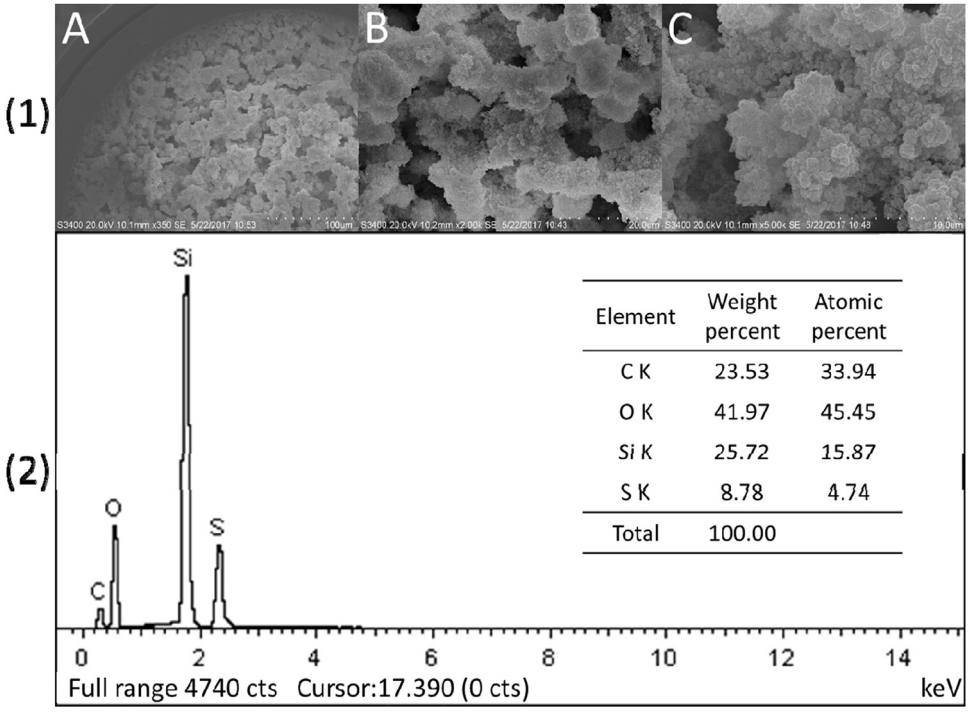

Fig. 6. SEM images (1) and EDS result (2) of the hybrid monolithic column. SEM: A. ×350; B. ×2.00k; C. ×5.00k.

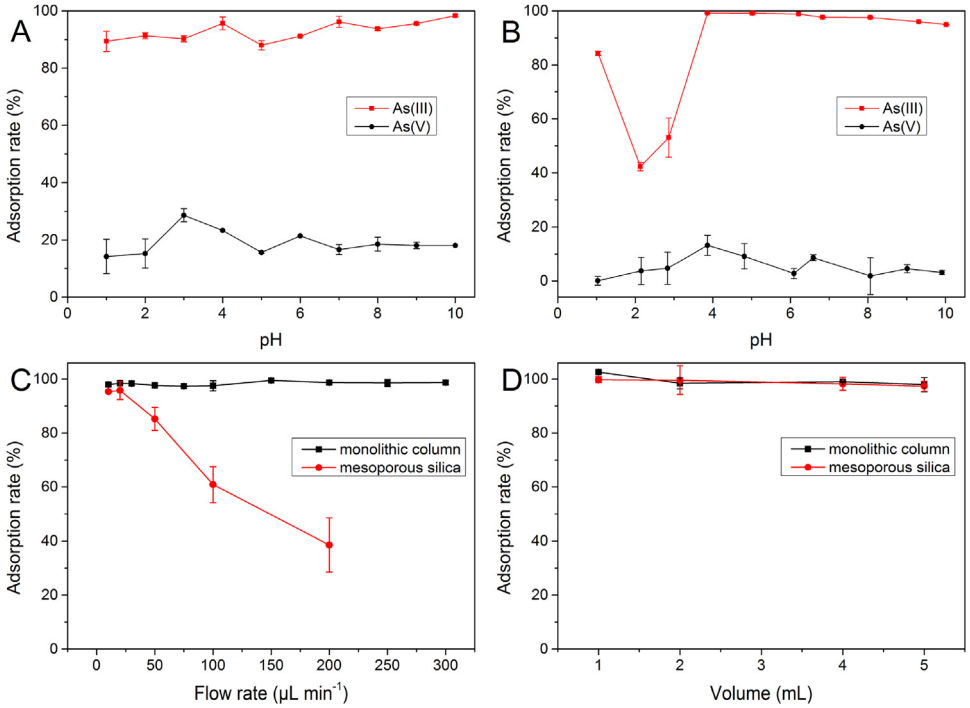

Fig. 7. Influence of sample pH on the adsorption of As(III) and As(V) by thiol-functionalized mesoporous silica (A) and thiol-functionalized monolithic column (B). Influence of flow rate (C) and sample volume (D) on the adsorption of As(III) by thiol-functionalized mesoporous silica and thiol-functionalized monolithic column.

3.2.5. Interference study

The interference effects of diverse ions on As(III) sorption onto the TFMS4 and monolith column were studied under the optimized conditions. Specifically, 1.0 mL sample solution containing 10 μg L^{-1} As (III) and a certain amount of interfering ions was allowed to flow through the filter disc and 5 cm monolithic capillary columns. The results, listed in Table S5, indicated that the adsorption rate for As(III) was still above 95% in the presence of 5 mg L^{-1} of Na^+, K^+ and Ca^{2+}, 1 mg L^{-1} of Mg^{2+}, Zn^{2+}, Al^{3+} and Ni^{2+}, 0.5 mg L^{-1} of Fe^{3+} and 0.1 mg L^{-1} of Cu^{2+} and Pb^{2+}. The adsorption rate did not change obviously when the main anions coexisted, such as 13 mg L^{-1} NO_3^-, 5 mg L^{-1} PO_4^{3-}, 4 mg L^{-1} SO_4^{2-} and 1 mg L^{-1} Cl^-. Therefore, other ions under the investigative concentration would not cause significant interference for the detection of As(III).

3.2.6. Eluent

The reason that As(III) was adsorbed by the two adsorbents was the strong chelation between mercapto groups and As(III). HNO_3 with 0.01 mol L^{-1} KIO_3 was employed to elute As(III) in reported works [9,37,38]. The effects of HNO_3 concentration and eluent volume were studied by continuously applying five replicates of 200 μL of eluents (0.01 mol L^{-1} KIO_3 dissolving in varying concentrations of HNO_3 from 3% to 10% (v/v)) to elute absorbed As(III). As can be seen from Fig. 8, all eluents with different HNO_3 concentration could achieve complete elution after two times (400 μL) for thiol-functionalized mesoporous silica, while 3% HNO_3 (v/v) with 0.01 mol L^{-1} KIO_3 performed better under less elution volume. In comparison, the different concentrations of HNO_3 had little significant effect on elution efficiency for thiol-functionalized monolithic capillary columns. Different from mesoporous materials, 200 μL eluent was sufficient for desorption of As(III) from the monolithic columns. Thus, 400 μL and 200 μL of eluent were applied to elute As(III) retained on two adsorbents respectively in environment water sample analysis.

3.3. Analytical performance and sample analysis

3.3.1. Analytical performance

Under the optimized condition, the analytical performance of the SPE/SPME-ICP-MS method, by taking thiol-functionalized mesoporous silica, TFMS4, and monolith column for adsorbents, were as follows:

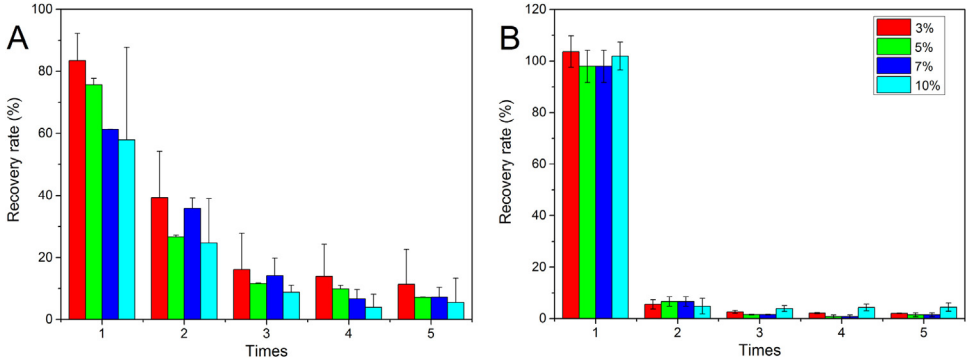

Fig. 8. Influence of different concentration and volume of HNO_3 with 0.01 mol L^{-1} KIO_3 solution (200 μL per time) on the desorption of As(III) from thiol-functionalized mesoporous silica (A) and thiol-functionalized monolithic column (B).

Table 2
Comparison of analytical performance obtained in this work with other adsorbents for the determination of As(III).

Adsorbent	Adsorption capacity	Analytical mode	Contact time (Flow rate)	Ref.
Activated red mud	0.8838	Batch SPE	1 h	[29]
iron oxide coated cement	0.69	Batch SPE	2 h	[30]
Chitosan resin	2.16	Batch SPE	8 h	[31]
Nanoscale zero-valent iron	3.50	Batch SPE	12 h	[32]
Thiol-activated alumina	11.53	Batch SPE	38 h	[33]
MPFS-PAA	0.093	Batch SPE	0.5 h	[34]
ZrO-EA	98.0	Batch SPE	50 min	[35]
(NH_2 + SH) modified silica gel	2.7	Batch SPE	30 min	[27]
Mercaptopropyl-mesostructured silica	~19.4	Batch SPE	> 20 h	[11]
Natural siderite	1.04	Batch/Column SPE	3 days	[36]
(NH_2 + SH) mesoporous silica	10.4	Batch/Syringe SPE	5 min (1 mL min^{-1})	[9]
MPTS-silica monolithic capillary	1.24[a]	On-line	(1 mL min^{-1})	[14]
DMSA-TiO_2	2.4	Micro-column SPE/On-line	(2 mL min^{-1})	[26]
Thiol-mesoporous silica	10.46	Syringe SPE	10 min (20 μL min^{-1})	This work
Thiol monolithic column	3.15 (2.43[a])	Needle SPE	(200 μL min^{-1})	This work

Unit of adsorption capacity: mg g^{-1}.
[a] μg cm^{-1}.

enrichment factor for As(III) onto the TFMS4 and monolith column were 10-fold and 20-fold. Furthermore, the calibration curves of As(III) in this work were established in the range of 0.2–50 μg L^{-1} with $r^2 > 0.998$ (for mesoporous silica) and $r^2 > 0.999$ (for monolithic column). The obtained limits of detection (LODs, defined as 3-fold signal-to-noise ratio) of As(III) onto the TFMS4 and monolith column were 0.05 and 0.025 μg L^{-1}, respectively, with the relative standard deviations (RSDs) of 9.1% and 5.0%, which was considerably lower than the allowed limit of arsenic in most drinking and environmental waters. In addition to this, the adsorbents (TFMS4 and monolith column) prepared within batch ($n = 3$) and between different batches ($n = 3$) were examined by measuring the recoveries of 20 μg L^{-1} As(III) solution under the optimized conditions. The stability of adsorbents was also examined using the adsorbents stored for different times (freshly-prepared, stored for one week and one month, $n = 3$). It was found that both TFMS4 and monolith column had good stability, repeatability and reproducibility (Table S6).

The comparison of analytical performance obtained in this present work with other adsorbents for the determination of As(III) is listed in Table 2. As can be seen, the adsorption capacities of both the adsorbents synthesized in this work were competitive comparing with other same types of materials, which demonstrated the superiority of application of TFMS4 and monolithic capillary columns on adsorption of As(III). Especially, the adsorption capacity of novel thiol-functionalized monolithic column synthesized *via* "one-step" was almost twice high than that of silica monolith column post-modified by mercapto groups. Most reported adsorbents need to take a long period of time to reach adsorption equilibrium in batch SPE process, while our mesoporous silica could reach the equilibrium in a relatively short time. It was easy to operate to use home-made syringe filter discs and monoliths as SPE/SPME devices instead of centrifuge for isolating the adsorbents from liquid samples. Meanwhile, the devices were very small, portable and suitable for on-site sampling and pre-treating environment waters, avoiding contamination and interference in shipping and storage. Comparing the thiol-functionalized mesoporous silica and monolithic columns in this work, monolithic column allowed for higher flow rate while maintaining adsorption efficiency, saving on analytical time for a single sample, which was more suitable for rapid sample analysis. However, without considering the time cost, the enrichment factor using mesoporous silica syringe filter disc could be enhanced by increasing the sample volume, therefore the mesoporous silica syringe filter disc would be a better choice under the condition of extremely low As(III) concentration in sample.

3.3.2. Sample analysis

In order to examine the feasibility of proposed methods, two kinds of environmental waters were used for the analysis of inorganic arsenic. As listed in Table 3, the experimental results obtained by thiol-functionalized mesoporous silica syringe filter discs and monolithic columns as SPE/SPME devices were in good agreement, with the recovery rate between 91–102% and 93–103% respectively, which indicated that the speciation analysis of inorganic arsenic in environmental samples could be achieved by the proposed methods.

Table 3
Determination of inorganic arsenic in environment water samples ($n = 4$).

Sample	Spiked level (μg L^{-1})		Found (μg L^{-1})		Recovery (%)	
	As(V)	As(III)	As(V)	As(III)	As(V)	As(III)
River water	0	0	0.58 ± 0.12 (0.60 ± 0.03)	2.68 ± 0.16 (2.71 ± 0.07)	–	–
	1.00	1.00	1.59 ± 0.15 (1.61 ± 0.02)	3.77 ± 0.11 (3.83 ± 0.06)	101 (101)	102 (103)
	2.00	2.00	2.50 ± 0.21 (2.53 ± 0.18)	4.62 ± 0.35 (4.80 ± 0.27)	97 (97)	99 (102)
Rain water	0	0	0.52 ± 0.13 (0.55 ± 0.01)	0.60 ± 0.09 (0.62 ± 0.03)	–	–
	1.00	1.00	1.39 ± 0.18 (1.44 ± 0.09)	1.51 ± 0.14 (1.56 ± 0.04)	91 (93)	94 (96)
	2.00	2.00	2.36 ± 0.25 (2.40 ± 0.13)	2.53 ± 0.30 (2.58 ± 0.26)	94 (94)	97 (98)

The result without brackets: using mesoporous silica as syringe SPE device.
The result in brackets: using monolithic column as needle SPME device.

4. Conclusions

In this work, thiol-functionalized mesoporous silica synthesized by "one-step" co-condensation was assembled into homemade syringe-based SPE device. At the same time, a novel thiol-functionalized monolithic SPME column was proposed in a novel ternary weak basic solvent system *via* "one-step" sol-gel process. Both two novel thiol-functionalized solid materials could capture As(III) in a wide pH range without uptaking As(V). The proposed SPE/SPME method with mesoporous silica syringe filter disc or monolithic column as extraction matrices possessed good separation and analysis performance for inorganic arsenic species, and very interestingly, could be applied to on-site sample pretreatment following collection of environment waters. Most importantly, discussing from the aspect of material preparation method, the abundant characterization results of mesoporous materials under the similar synthetic conditions provided vital reference and theoretical support for the synthesis of monolithic columns. However,

compared with mesoporous silica syringe filter disc, the monoliths showed more excellent performance used for inorganic arsenic speciation analysis in the matter of selective adsorption of As(III) and flow rate. As far as we know, this work is the first time to compare and relate two similar solid materials, mesoporous silica and monolithic column, and puts forward a feasible strategy for exploring the preparation conditions of novel organic-inorganic hybrid monolithic columns.

Acknowledgements

This work was supported by the National Natural Science Foundation of China (21577057, 91643105 and 91543129), the Natural Science Foundation of Jiangsu Province (BK20171335), the Environmental Monitoring Foundation of Jiangsu Province (1409), and the Analysis & Test Fund of Nanjing University.

Conflict of interest

The authors declare that they have no conflict of interest.

Appendix A. Supplementary material

Supplementary data associated with this article can be found in the online version at doi:10.1016/j.talanta.2018.07.034.

References

[1] G.K. Zoorob, J.W. Mckiernan, J.A. Caruso, ICP-MS for elemental speciation studies, Microchim. Acta 128 (1998) 145–168.
[2] E.G. Duncan, W.A. Maher, S.D. Foster, F. Krikowa, C.A. O'Sullivan, M.M. Roper, Dimethylarsenate (DMA) exposure influences germination rates, arsenic uptake and arsenic species formation in wheat, Chemosphere 181 (2017) 44–54.
[3] Q. Hu, Y. Liu, X. Gu, Y. Zhao, Adsorption behavior and mechanism of different arsenic species on mesoporous $MnFe_2O_4$ magnetic nanoparticles, Chemosphere 181 (2017) 328–336.
[4] T. Sun, Z. Zhao, Z. Liang, J. Liu, W. Shi, F. Cui, Efficient removal of arsenite through photocatalytic oxidation and adsorption by ZrO_2-Fe_3O_4 magnetic nanoparticles, Appl. Surf. Sci. 416 (2017) 656–665.
[5] R.R. Shrestha, M.P. Shrestha, N.P. Upadhyay, R. Pradhan, R. Khadka, A. Maskey, M. Maharjan, S. Tuladhar, B.M. Dahal, K. Shrestha, Groundwater arsenic contamination, its health impact and mitigation program in Nepal, J. Environ. Sci. Heal. A 38 (1) (2003) 185–200.
[6] R. Yang, Y. Su, K.B. Aubrecht, X. Wang, H. Ma, R.B. Grubbs, B.S. Hsiao, B. Chu, Thiol-functionalized chitin nanofibers for As(III) adsorption, Polymer 60 (2015) 9–17.
[7] Y. Xiong, Q. Tong, W. Shan, Z. Xing, Y. Wang, S. Wen, Z. Lou, Arsenic transformation and adsorption by iron hydroxide/manganese dioxide doped straw activated carbon, Appl. Surf. Sci. 416 (2017) 618–627.
[8] L. Xu, Z.G. Shi, Y.Q. Feng, Porous monoliths: sorbents for miniaturized extraction in biological analysis, Anal. Bioanal. Chem. 399 (2011) 3345–3357.
[9] P. Li, X.Q. Zhang, Y.J. Chen, T.Y. Bai, H.Z. Lian, X. Hu, One-pot synthesis of thiol- and amine-bifunctionalized mesoporous silica and applications in uptake and speciation of arsenic, RSC Adv. 4 (2014) 49421–49428.
[10] H. Shirkhanloo, M. Ghazaghi, A. Rashidi, A. Vahid, Arsenic speciation based on amine-functionalized bimodal mesoporous silica nanoparticles by ultrasound assisted-dispersive solid-liquid multiple phase microextraction, Microchem. J. 130 (2017) 137–146.
[11] E. McKimmy, J. Dulebohn, J. Shah, T.J. Pinnavaia, Trapping of arsenite by mercaptopropyl-functionalized mesostructured silica with a wormhole framework, Chem. Commun. 29 (2005) 3697–3699.
[12] J. Aguado, J.M. Arsuaga, A. Arencibia, M. Lindo, V. Gascón, Aqueous heavy metals removal by adsorption on amine-functionalized mesoporous silica, J. Hazard. Mater. 163 (2009) 213–221.
[13] L.Y. Yuan, Z.Q. Bai, R. Zhao, Y.L. Liu, Z.J. Li, S.Q. Chu, L.R. Zheng, J. Zhang, Y.L. Zhao, Z.F. Chai, W.Q. Shi, Introduction of bifunctional groups into mesoporous silica for enhancing uptake of thorium(IV) from aqueous solution, ACS Appl. Mater. Interfaces 6 (2014) 4786–4796.
[14] F. Zheng, B. Hu, Dual silica monolithic capillary microextraction (CME) on-line coupled with ICP-MS for sequential determination of inorganic arsenic and selenium species in natural waters, J. Anal. At. Spectrom. 24 (2009) 1051–1061.
[15] L. Zhang, B. Chen, M. He, B. Hu, Polymer monolithic capillary microextraction combined on-line with inductively coupled plasma MS for the determination of trace rare earth elements in biological samples, J. Sep. Sci. 36 (2013) 2158–2167.
[16] Y. Cai, B. Chen, M. He, X. Liu, H. Bin, Gold nanoparticles as intermediate ligands for polymer monolithic capillary microextraction of trace rare earth elements followed by inductively coupled plasma mass spectrometry detection, Spectrochim. Acta B 127 (2017) 56–63.
[17] X. Liu, B. Chen, L. Zhang, S. Song, Y. Cai, M. He, B. Hu, TiO_2 nanoparticles functionalized monolithic capillary microextraction online coupled with inductively coupled plasma mass spectrometry for the analysis of Gd ion and Gd-based contrast agents in human urine, Anal. Chem. 87 (2015) 8949–8956.
[18] J.C. Zhao, Q.Y. Zhu, L.Y. Zhao, H.Z. Lian, H.Y. Chen, Preparation of an aptamer based organic-inorganic hybrid monolithic column with gold nanoparticles as an intermediary for the enrichment of proteins, Analyst 141 (2016) 4961–4967.
[19] J. Lu, F. Ye, A. Zhang, Z. Wei, Y. Peng, S. Zhao, Preparation and characterization of silica monolith modified with bovine serum albumin-gold nanoparticles conjugates and its use as chiral stationary phases for capillary electrochromatography, J. Sep. Sci. 34 (2011) 2329–2336.
[20] C. Xie, J. Hu, H. Xiao, X. Su, J. Dong, R. Tian, Z. He, H. Zou, Preparation of monolithic silica column with strong cation-exchange stationary phase for capillary electrochromatography, J. Sep. Sci. 28 (2005) 751–756.
[21] P. Scholder, M. Hafner, A.W. Hassel, I. Nischang, Gold nanoparticle@polyhedral oligomeric silsesquioxane hybrid scaffolds in microfluidic format – highly efficient and green catalytic platforms, Eur. J. Inorg. Chem. 2016 (2016) 951–955.
[22] L. Xu, H.K. Lee, Preparation, characterization and analytical application of a hybrid organic-inorganic silica-based monolith, J. Chromatogr. A 1195 (2008) 78–84.
[23] H. Yang, Y. Chen, Y. Liu, L. Nie, S. Yao, One-pot synthesis of (3-sulfopropyl methacrylate potassium)-silica hybrid monolith *via* thiol-ene click chemistry for CEC, Electrophoresis 34 (2013) 510–517.
[24] X. Lv, W. Tan, Y. Chen, Y. Chen, M. Ma, B. Chen, S. Yao, Facile "one-pot" synthesis of poly(methacrylic acid)-based hybrid monolith *via* thiol-ene click reaction for hydrophilic interaction chromatography, J. Chromatogr. A 1454 (2016) 49–57.
[25] P. Li, X.Q. Zhang, Y.J. Chen, H.Z. Lian, X. Hu, A sequential solid phase microextraction system coupled with inductively coupled plasma mass spectrometry for speciation of inorganic arsenic, Anal. Methods 6 (2014) 4205–4211.
[26] C. Huang, B. Hu, Z. Jiang, Simultaneous speciation of inorganic arsenic and antimony in natural waters by dimercaptosuccinic acid modified mesoporous titanium dioxide micro-column on-line separation and inductively coupled plasma optical emission spectrometry determination, Spectrochim. Acta B 62 (2007) 454–460.
[27] E. Boyacı, A. Çağır, T. Shahwan, A.E. Eroğlu, Synthesis, characterization and application of a novel mercapto- and amine-bifunctionalized silica for speciation/sorption of inorganic arsenic prior to inductively coupled plasma mass spectrometric determination, Talanta 85 (2011) 1517–1525.
[28] W.L. Hu, B. Hu, Z.C. Jiang, On-line preconcentration and separation of Co, Ni and Cd via capillary microextraction on ordered mesoporous alumina coating and determination by inductively plasma mass spectrometry (ICP-MS), Anal. Chim. Acta 572 (2006) 55–62.
[29] H.S. Altundoğan, S. Altundoğan, F. Tümen, M. Bildik, Arsenic adsorption from aqueous solutions by activated red mud, Waste Manag. 22 (2002) 357–363.
[30] S. Kundu, A.K. Gupta, Adsorption characteristics of As(III) from aqueous solution on iron oxide coated cement (IOCC), J. Hazard. Mater. 142 (2007) 97–104.
[31] B. Liu, X. Lv, D. Wang, Y. Xu, L. Zhang, Y. Li, Adsorption behavior of As(III) onto chitosan resin with As(III) as template ions, J. Appl. Polym. Sci. 125 (2012) 246–253.
[32] S.R. Kanel, B. Manning, L. Charlet, H. Choi, Removal of arsenic(III) from groundwater by nanoscale zero-valent iron, Environ. Sci. Technol. 39 (2005) 1291–1298.
[33] J. Hao, M.J. Han, X. Meng, Preparation and evaluation of thiol-functionalized activated alumina for arsenite removal from water, J. Hazard. Mater. 167 (2009) 1215–1221.
[34] R. Kumar, S.K. Jain, S. Verma, P. Malodia, Mercapto functionalized silica entrapped polyacrylamide hydrogel: arsenic adsorption behaviour from aqueous solution, J. Colloid Interface Sci. 456 (2015) 241–245.
[35] S. Mandal, T. Padhi, R.K. Patel, Studies on the removal of arsenic (III) from water by a novel hybrid material, J. Hazard. Mater. 192 (2011) 899–908.
[36] H. Guo, D. Stüben, Z. Berner, Adsorption of arsenic(III) and arsenic(V) from groundwater using natural siderite as the adsorbent, J. Colloid Interface Sci. 315 (2007) 47–53.
[37] W.W. Bennett, M. Arsic, D.T. Welsh, P.R. Teasdale, *In situ* speciation of dissolved inorganic antimony in surface waters and sediment porewaters: development of a thiol-based diffusive gradients in thin films technique for Sb^{III}, Environ. Sci. Process. Impacts 18 (2016) 992–998.
[38] W.W. Bennett, P.R. Teasdale, J.G. Panther, D.T. Welsh, D.F. Jolley, Speciation of dissolved inorganic arsenic by diffusive gradients in thin films: selective binding of As^{III} by 3-mercaptopropyl-functionalized silica gel, Anal. Chem. 83 (2011) 8293–8299.